Self-Assembly and Fluorescent Modification of Hydroxyapatite Nanoribbon Spherulites

Jinku Liu,[a] Qingsheng Wu,*[a] and Yaping Ding*[b]

Keywords: Fluorescence / Hydroxyapatite / Nanostructures / Self-assembly

Hydroxyapatite nanoribbon spherulites have been successfully synthesized, with the bioactive eggshell membrane as directing template and in the presence of ethylenediamine, in a one-step reaction under mild conditions. The spherulites are about 2.5 μm in diameter and the extended nanoribbon about 1.1 μm long. The spherulites were modified with fluorescein to obtain a fluorescent probe material with strong luminescence.

Introduction

Assembly of nanocrystals to form ordered structures is of great interest in the area of materials science. The ability to synthesize uniformly assembled nanospheres with diameters ranging from nano- to microscale dimensions is especially desirable[1] as these structures can be used in therapeutic, storage, and catalytic fields[2,3] etc.[4] Ribbon-shaped nanomaterials or nanostructures have attracted a great deal of attention since the discovery of zinc oxide nanobelts in 2001 by Wang,[5] and the assembly of materials/structures is still an important objective. Up to now, the obtained inorganic nanobelts/nanoribbons mainly include oxides,[5–7] elementary substances,[8–10] sulfides,[11,12] etc.,[13–16] and no study has been reported on the formation of hydroxyapatite nanoribbons. On the other hand, although various spherical nano-/micromaterials have been reported, they are mainly solid[17–22] or hollow.[23–33]

In this paper, a novel assembly method for nanomaterials, which includes a bioactive eggshell membrane[34] template approach with the cooperative effect of ethylenediamine, is developed that gives hydroxyapatite nanoribbon spherulites in a single-step reaction at room temperature. The obtained spherulites can be modified with fluorescein to form spherical fluorescent probe materials with strong luminescence. The hydroxyapatite spherulites have attracted a good deal of attention as a delivery system because of their special physical and chemical properties, high surface-interaction properties, and their biocompatibility. Therefore, these nanoribbon spherulites have potential value in biology, medicine, and drug fields etc.

[a] Department of Chemistry, Tongji University, Shanghai 200092, China
Fax: +86-021-6598-2287
E-mail: qswu@mail.tongji.edu.cn
[b] Department of Chemistry, Shanghai University, Shanghai 200444, China
E-mail: ypding@mail.shu.edu.cn

Results and Discussion

All the XRD diffraction patterns in Figure 1 can be readily indexed to a hydroxyapatite [$Ca_5(PO_4)_3(OH)$] phase, and there is an obvious indication of the crystal growth direction in the XRD pattern. The XRD analysis was repeated several times with similar results: the 002 diffraction looks rather sharp and intense, indicating a non-nanoscale and good crystallization at the 002 crystal face, while the other diffractions look broad, indicating a nanoscale and a poorer crystallization. According to the product's morphology and XRD results, the most likely growth direction of the nanoribbons is on the [002] crystal face.

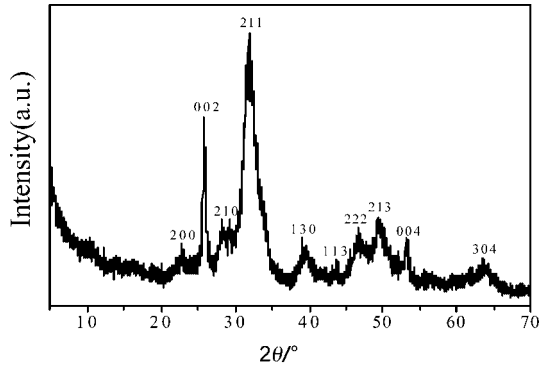

Figure 1. The XRD pattern of hydroxyapatite nanoribbon spherulites.

Figure 2 also shows a similar widening in the FT-IR absorption peaks. The ν_{P-O} vibration of the hydroxyapatite nanoribbon spherulites in Figure 2 (b) is at almost the same wavelength as that of hydroxyapatite bulk materials in Figure 2 (a) (1040 cm^{-1}), although it is obviously wider. This may be because the small-size effects and interface effects of nanomaterials change the ν_{P-O} vibration energy.

 DOI: 10.1002/ejic.200500207

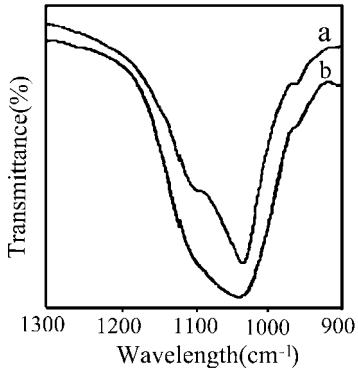

Figure 2. The FT-IR spectrum of products (a: bulk materials; b: spherulites).

The hydroxyapatite nanoribbon spherulites are different from hollow spherulites and solid spheres as the spherulites are in fact built from interlaced nanoribbons. Figure 3 (see part a) shows a typical TEM image of the products, which shows that they are spherulites with a diameter of about 2.5 μm. The high magnification TEM image in Figure 3 (part b) indicates that the spherulites consist of a large number of nanoribbons, the thickness and width of which are about 8 nm and 200 nm respectively; the length of the extended nanoribbons is about 1.1 μm. The electron diffraction (ED) lattice of a selected region suggests that the nanoribbons are single crystals (Figure 3, c). The obtained spherulites are porous structures composed of nanoribbons. They have a large surface area that contains a large number of hydroxy groups. With such a structure, they can easily combine with organic fluorescent compounds that contain carboxyl or hydroxy groups.

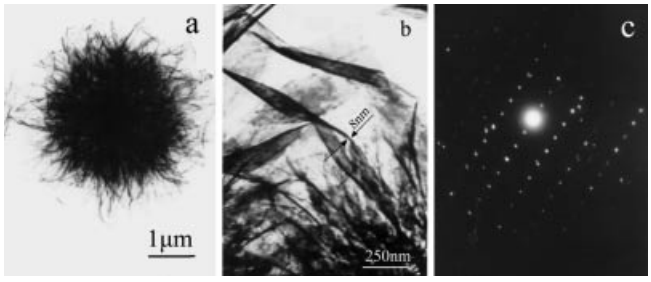

Figure 3. TEM and ED images of the products.

When irradiated with an electron beam, the hydroxyapatite nanoribbon spherulites change into a solid sphere. Figure 4 (a) shows the TEM image of a spherulite with a diameter of about 2.5 μm before irradiation. After irradiation with an electron beam for several seconds the product changes into a solid sphere with a diameter of 2.3 μm (Figure 4, b) consisting of melted hydroxyapatite. This can be explained by the fact that hydroxyapatite has a high chemical stability,[35] therefore decomposition cannot occur at the irradiation temperature of the electron beam[36] and it only melts.

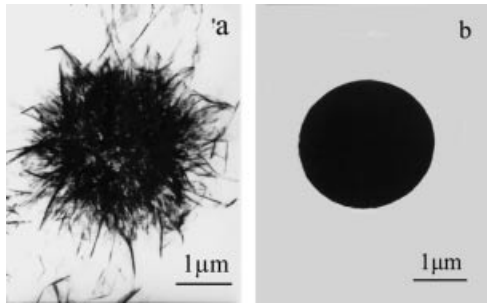

Figure 4. TEM images of the products (a: nanoribbon spherulite; b: solid sphere).

The growth processes of hydroxyapatite spherulites were determined by examining different stages of their formation. As shown in Figure 5a, nanoribbons with lengths ranging from 200 to 250 nm have formed after 0.5 h of aging, and they distributed randomly. After aging for 4 h, the products are approximately spherical with a diameter of 1.9 μm, as shown in part b of Figure 5, which suggests that the nanoribbons are not yet completely assembled and the spherulites are rather loose. When the aging time was further increased to 10 h, integrated spherical hydroxyapatite appeared, but the extended nanoribbons were still a little longer. They continued to become larger and more compact with time, and when the aging time reached two days, very compact spherulites had formed whose extended nanoribbons are shorter (200 nm; Figure 5, d). Even after aging for four days (further aging leads to the decomposition of the eggshell membrane), the final products were still hydroxyapatite nanoribbon spherulites similar to that in Figure 5, part d; no solid spherulite was obtained. These results indicate that shorter nanoribbons form at first, and then these assemble gradually to form many spherulite cores. Thereafter, the nanoribbons continue to assemble around the cores to form many large and compact spherulites.

The most suitable temperature for the formation of spherical hydroxyapatite is 37 °C, which is approximately physiological temperature. When the reaction was performed at a lower temperature (0 °C for 10 h) spherical hydroxyapatite also formed, as shown in Figure 6, but with a diameter of about 1.6 μm, far smaller than that at 37 °C. This may be explained by considering that the low temperature slows down diffusion of the ions and therefore assembly of the nanoribbons, and the eggshell membrane has lower activity at 0 °C than at physiological temperature, whichl weakens its inducing ability foro the formation of spherical hydroxyapatite.

The hydroxyapatite nanoribbons assemble into spherulites by an organic direction process.[22,23,37–39] This process is induced under the cooperative effect of the eggshell membrane and ethylenediamine. A TEM image in which the spherulites and the intermediate products exist simultaneously was taken during the experiment, as shown in Figure 7, from which a conjecture can be made that the spherulite cores marked with an arrow are assembled from a small

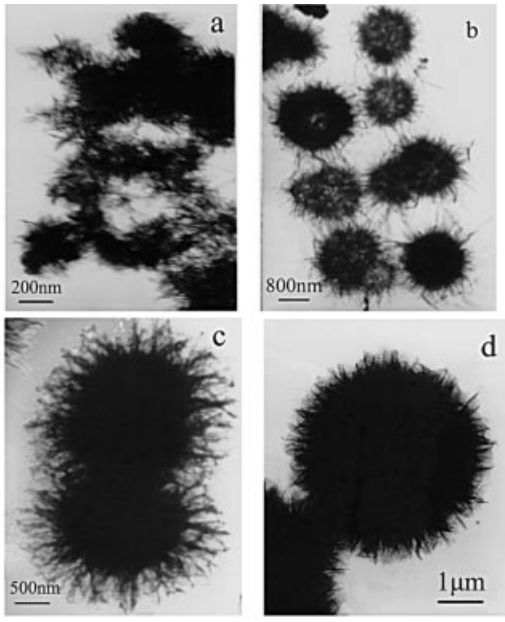

Figure 5. TEM images of the products [aging time: 1 h (a); 4 h (b); 10 h (c); 2 d (d)].

Figure 6. TEM pattern of the products obtained at 0 °C (aging for 10 h).

quantity of nanoribbons formed during the first step, and then these spherulite cores assemble into nanoribbon spherulites. Figure 8 shows a typical scanning electron microscopy (SEM) image of the eggshell membrane. The eggshell membrane is a microporous network with diameters of 1.5–10 μm, which is composed of interlaced protein fibers with an average diameter of about 2 μm. The eggshell membrane mainly contains collagens, glycoproteins, and proteoglycans. These macromolecules contain a large amount of amido, carboxy, and hydroxy groups, and have both hydrophilic and hydrophobic domains located at their ends.[40] The hydrophobic domains extend onto the surface of the crystal and block diffusion of the lattice ions to the crystal surface. The ethylenediamine acts as an additional template due to hydrogen-bonding effects between its NH_2 groups and the surface groups of the eggshell membrane such as COOH and NH_2. The products are obtained on either side of the eggshell membrane, which indicates that the products fall randomly from the template.

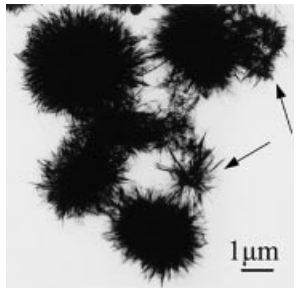

Figure 7. The SEM pattern of spherulites and intermediate products (after aging for 2 d).

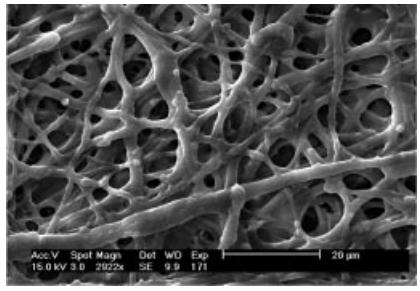

Figure 8. The SEM pattern of eggshell membrane.

As a template, the eggshell membrane has an effect in three aspects. Firstly, it can control the transport of ions due to its semi-permeable structure. Secondly, it not only can alone induce the formation of products, but can also interact with ethylenediamine through hydrogen bonds and consequently control the growth of products. Finally, the eggshell membrane offers a physical site in the hole channels of which the two kinds of ions meet, react, aggregate to form a crystal nucleus, and then grow under the control of the eggshell membrane and ethylenediamine to form the products. Moreover, it must be emphasized that the template used in this paper is not a simple flat structure. Rather, it is composed of macromolecules on the surface of curving hole channels of the eggshell membrane and ethylenediamine, which cooperatively form a spherical template and control the growth of hydroxyapatite nanoribbon spherulites. The nanoribbon spherulites can't be obtained in the absence of the eggshell membrane (Figure 9, a).

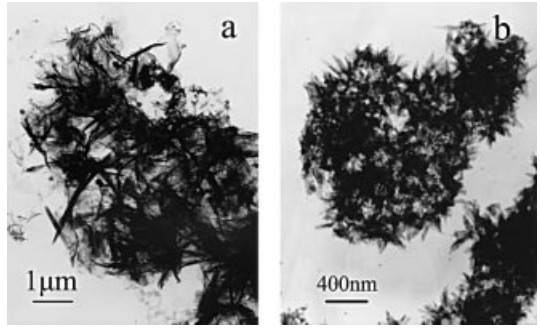

Figure 9. TEM images of the products (a: when the eggshell membrane is absent; b: when KOH was added to adjust the pH to 7.4).

The organic base ethylenediamine is employed here to modulate the pH value to 7.4 and spherical products were obtained. When potassium hydroxide was used instead, the products were sparse flakes of hydroxyapatite about 300 nm long, as shown in part b of Figure 9. This indicates that the organic base plays an important role in the controllable assembly of spherical products. The morphological difference in the presence of inorganic and organic base is because, besides the adjusting pH value, ethylenediamine also acts as an accessorial template due to hydrogen-bonding effects between its NH_2 groups and the surface groups of the eggshell membrane such as COOH, NH_2.

The hydroxyapatite nanoribbon spherulites form as follows. First, the two reacting ions meet and react in the hole channels of the eggshell membrane. The formed $Ca_5(PO_4)_3$-OH molecules then aggregate to form a crystal nucleus, which grows under the cooperative control of the eggshell membrane and ethylenediamine on the surface of the eggshell membrane to form hydroxyapatite nanoribbon spherulites. The formed nanoribbon spherulites fall from the eggshell membrane into the solution due to the pressure of the diffused reaction ions, the newly formed products, gravity, and thermal motion.

The hydroxyapatite nanoribbon spherulites were treated with fluorescein, $C_{20}H_{12}O_5$, which is a fluorescent molecule whose structural formula is shown in Scheme 1. The TEM images of the resulting fluorescent probe materials (Figure 10, a) indicate that they are spherical with a diameter of about 2.1 μm, which is less than that of the unmodified products. This can be explained by supposing that the close combination of fluorescein and hydroxyapatite nanoribbon spherulites, mainly through two kinds of strong effects, reduces the diameter. As the hydroxyapatite nanoribbon spherulite is a porous structure composed of interlaced nanoribbons, one of these effect is likely to be hydrogen bonding between the hydroxy groups in the hydroxyapatite spherulite and the COOH, OH, and C=O groups of fluorescein. The other is the strong surface adsorption ability of hydroxyapatite spherulites to fluorescein molecules due to its large surface area. It is these two effects that combine the fluorescein and nanoribbon spherulite tightly. The TEM images show that the nanoribbons have almost disappeared, the surface is smooth, and there is appreciable darkness in the center, as indicated by the arrow in Figure 10 (b), which suggests that, instead of just adhering to the spherulite surface, fluorescein is embedded inside the spherulites.

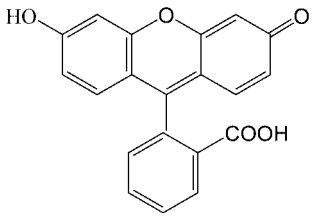

Scheme 1. Structure of fluorescein.

The modified products were rinsed several times with ethanol to exclude the possibility that fluorescein just clings

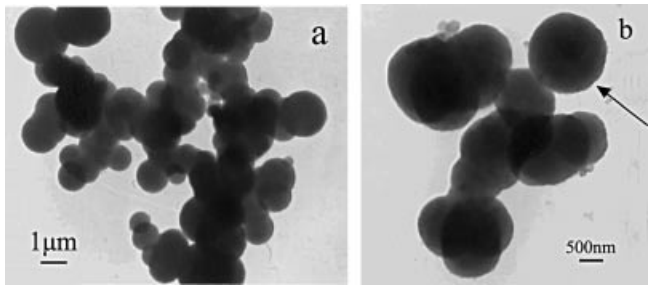

Figure 10. The TEM pattern of products modified with fluorescein.

to the surface of the fluorescent probe materials. The fluorescence spectra of unmodified and modified products indicate that nanoribbon spherulites are not photoluminescent, as shown in Figure 11 (c), whereas Figure 11 (b) shows that the luminescence of the modified products is very strong. At an excitation wavelength of 314 nm, the fluorescent probe materials emit green lighty of 514 nm (Figure 11, b), slightly different from the emission wavelength of the nanoribbon spherulites (511nm; Figure 11, a). This is because the interaction between the nanoribbons and fluorescein changes the ligand field of fluorescein and thus alters the electron distribution in the conjugated system of fluorescein molecules, which results in a change of the transition bandgaps of the electrons. Moreover, the XRD pattern of the modified product (Figure 12, a) shows that it is also a

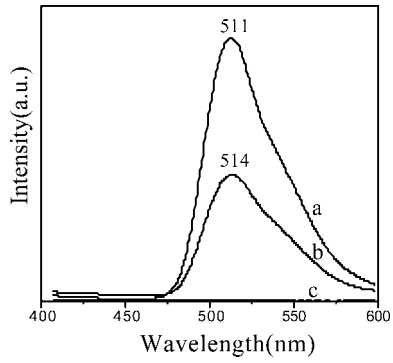

Figure 11. The fluorescence spectra of the products (a: fluorescein; b: fluorescent probe materials; c: nanoribbon spherulites. Excitation wavelength: 383 nm).

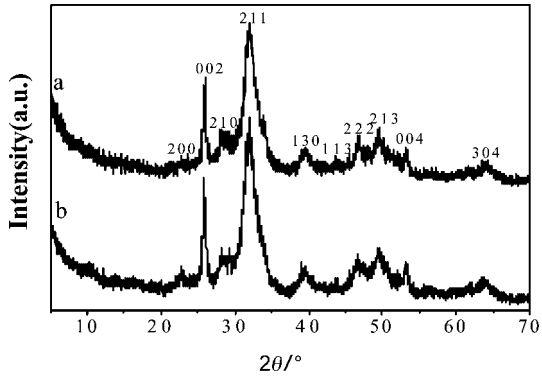

Figure 12. The XRD pattern of modified products (a: modified products; b: nanoribbon spherulites).

hydroxyapatite structure, which indicates that hydroxyapatite combines with the fluorescein through nonchemical bonds, such as hydrogen bonds.

Conclusion

Hydroxyapatite spherulites assembled from long nanoribbons have been synthesized in a one-step reaction at room temperature with a novel bioactive eggshell membrane as the template and in the presence of ethylenediamine. This porous spherulite can be transformed into a solid one by electron beam irradiation. It can also combine with some organic compounds through hydrogen bonding and surface adsorption effects. Based on these properties, a fluorescent probe material with hydroxyapatite nanoribbons spherulites as substrates has been successfully prepared, and it provides a novel idea for the application of assembling nanoribbon spherulites in medical, biological, and industrial fields.

Experimental Section

The eggshell membrane was taken from a fresh eggshell after removing the outer shell and washing with deionized water. It was then fastened in a container to separate it into two horizontal compartments into which 20 mL of 0.1 M $CaCl_2$ and 20 mL of 0.06 M KH_2PO_4 were added, respectively. Ethylenediamine was put in both sides of the membrane to modulate the pH value to 7.4. All reagents used were of analytical purity. Thereafter, the reaction container was kept at 37 °C for ten hours. The obtained products were separated in a centrifuge at 1500 rpm and washed with deionized water and alcohol several times, one after the other, until no Ca^{2+} and ethylenediamine could be detected. The washed products were collected and dried in a desiccator to give the final products.

A sample of the above products (0.5 g) was put in 50 mL of a 2% aqueous fluorescein solution, the system was vibrated ultrasonically for 20 min, and then separated. The precipitates were rinsed with ethanol to remove the excessive fluorescein until the ethanol solution showed no fluorescence by fluorescent spectroscopy. Then, the washed products were collected and dried in a desiccator to obtain the final modified products.

The morphologies of the products were observed by transmission electron microscopy (TEM). The crystal phase and structure of the products were determined by X-ray powder diffraction (XRD) using a Shimadzu XD-3A diffractometer with graphite-monochromated Cu-K_α radiation (50 kV, 100 mA). The optical properties of the products were studied by FT-IR spectroscopy and fluorescent spectroscopy (Perkin–Elmer LS-55).

Acknowledgments

This work was supported by the National Natural Science Foundation of China (grant nos. 20471042 and 20131030), the Nano Foundation of Shanghai (grant nos. 0452nm075 and 0352nm129), and the Doctoral Program Foundation of the Ministry of Education of China (grant no. 20040247045).

[1] J. K. Yuan, K. Laubernds, Q. H. Zhang, S. L. Suib, *J. Am. Chem. Soc.* **2003**, *125*, 4966.
[2] F. Caruso, R. A. Caruso, H. Mohwald, *Science* **1998**, *282*, 1111.
[3] H. W. Duan, D. Y. Chen, M. Jiang, W. J. Gan, S. J. Li, M. Wang, J. Gong, *J. Am. Chem. Soc.* **2001**, *123*, 12097.
[4] C. F. Wang, S. Y. Xie, S. C. Lin, X. Cheng, X. H. Zhang, R. B. Huang, L. S. Zheng, *Chem. Commun.* **2004**, *15*, 1766.
[5] Z. W. Pan, Z. R. Dai, Z. L. Wang, *Science* **2001**, *291*, 1947.
[6] X. L. Li, Y. D. Li, *Chem. Eur. J.* **2003**, *9*, 2726.
[7] A. Maiti, J. A. Rodriguez, M. Law, P. Kung, J. R. Mckinney, P. D. Yang, *Nano Lett.* **2003**, *3*, 1025.
[8] X. B. Cao, Y. Xie, S. Y. Zhang, F. Q. Li, *Adv. Mater.* **2004**, *16*, 649.
[9] Y. G. Sun, B. Mayers, Y. N. Xia, *Nano. Lett.* **2003**, *3*, 675.
[10] A. Swami, A. Kumar, P. R. Selvakannan, S. Mandal, R. Pasricha, M. Sastry, *Chem. Mater.* **2003**, *15*, 17.
[11] J. Zhang, F. H. Jiang, L. D. Zhang, *J. Phys. Chem. B* **2004**, *108*, 7002.
[12] Z. P. Liu, S. Peng, Q. Xie, Z. K. Hu, Y. Yang, S. Y. Zhang, Y. T. Qian, *Adv. Mater.* **2003**,*15*, 936.
[13] C. Ma, Y. Ding, D. Moore, X. D. Wang, Z. L. Wang, *J. Am. Chem. Soc.* **2004**, *126*, 708.
[14] H. T. Shi, L. M. Qi, J. M. Ma, H. M. Cheng, B. Y. Zhu, *Adv. Mater.* **2003**,*15*, 1647.
[15] Y. Jiang, X. M. Meng, W. C. Yiu, J. Liu, J. X. Ding, C. S. Lee, S. T. Lee, *J. Phys. Chem. B* **2004**, *108*, 784.
[16] X. T. Zhang, J. Zhang, Z. F. Liu, C. Robinson, *Chem. Commun.* **2004**, *16*, 1852.
[17] S. H. Yu, H. Cölfen, A. W. Xu, W. F. Dong, *Cryst. Growth Des.* **2004**, *4*, 33.
[18] L. E. Euliss, T. M. Trnka, T. J. Deming, G. D. Stucky, *Chem. Commun.* **2004**, *15*, 1736.
[19] C. Z. Wu, Y. Xie, D. Wang, J. Yang, T. W. Li, *J. Phys. Chem. B* **2003**, *107*, 13583.
[20] S. H. Rheel, J. Tanaka, *Biomaterials* **1999**, *20*, 2155.
[21] M. S. Fleming, T. K. Mandal, D. R. Walt, *Chem. Mater.* **2001**, *13*, 2210.
[22] X. M. Sun, Y. D. Li, *Angew. Chem. Int. Ed.* **2004**, *43*, 597.
[23] Q. Peng, Y. J. Dong, Y. D. Li, *Angew. Chem. Int. Ed.* **2003**, *42*, 3027.
[24] J. X. Huang, Y. Xie, B. Li, Y. Liu, Y. T. Qian, S. Y. Zhang, *Adv. Mater.* **2000**, *12*, 808.
[25] B. Liu, H. C. Zeng, *J. Am. Chem. Soc.* **2004**, *126*, 8124.
[26] N. Bowden, A. Terfort, J. Carbeck, G. M. Whitesides, *Science* **1997**, *276*, 233.
[27] H. Cölfen, S. Mann, *Angew. Chem. Int. Ed.* **2003**, *42*, 2350.
[28] J. C. Love, A. R. Urbach, M. G. Prentiss, G. M. Whitesides, *J. Am. Chem. Soc.* **2003**, *125*, 12696.
[29] G. M. Whitesides, B. Grzybowski, *Science* **2002**, *295*, 2418.
[30] K. P. Velikov, C. G. Christova, R. P. A. Dullens, V. A. Blaaderen, *Science* **2002**, *296*, 106.
[31] P. Yang, *Nature* **2003**, *425*, 243.
[32] S. Park, J. H. Lim, S. W. Chung, C. A. Mirkin, *Science* **2004**, *303*, 348.
[33] M. Antonietti, M. Breulmann, C. G. Göltner, H. Cölfen, K. K. W. Wong, D. Walsh, S. Mann, *Chem. Eur. J.* **1998**, *4*, 2493.
[34] D. Yang, L. M. Qi, J. M. Ma, *Adv. Mater.* **2002**, *14*, 1543.
[35] T. Hirai, M. Hodono, I. Komasawa, *Langmuir* **2000**, *16*, 955.
[36] Y. D. Li, J. W. Wang, Z. X. Deng, Y. Y. Wu, X. M. Sun, D. P. Yu, P. D. Yang, *J. Am. Chem. Soc.* **2001**, *123*, 9904.
[37] C. Pacholski, A. Kornowski, H. Weller, *Angew. Chem. Int. Ed.* **2002**, *41*, 1188.
[38] X. W. Lou, H. C. Zeng, *J. Am. Chem. Soc.* **2003**, *125*, 2697.
[39] H. T. Shi, L. M. Qi, J. M. Ma, H. M. Cheng, *Chem. Commun.* **2002**, *16*, 1704.
[40] P. K. Ajikumar, R. Lakshminarayanan, B. T. Ong, S. Valiyaveettil, R. M. Kini, *Biomacromolecules* **2003**, *4*, 1321.

Received: March 8, 2005
Published Online: September 13, 2005

